

Measurement of the total neutron cross section on argon in the 20 to 70 keV energy range

S. Andringa,¹ Y. Bezawada,² T. Erjavec,² J. He,² J. Huang,² P. Koehler,³ M. Mocko,³ M. Mulhearn,² L. Pagani,² E. Pantic,² L. Pickard,² R. Svoboda,² J. Ullmann,³ and J. Wang^{2,4}

(ARTIE Collaboration)

¹*Laboratório de Instrumentação e Física Experimental de Partículas (LIP),
Av. Prof. Gama Pinto, 2, 1649-003, Lisboa, Portugal*

²*University of California at Davis, Department of Physics and Astronomy, Davis, CA 95616, U.S.A.*

³*Los Alamos National Laboratory, Physics Division, Los Alamos, NM 87545, U.S.A.*

⁴*South Dakota School of Mines and Technology, Physics Department, Rapid City, SD 57701 USA
(Dated: December 13, 2022)*

The cross section for neutron interactions on argon is an important design and operational parameter for a number of neutrino, dark matter, and neutrinoless double beta decay experiments which use liquid argon as a detection or shielding medium. There is a discrepancy between the total cross section in the 20 to 70 keV neutron kinetic energy region given in the ENDF database and a single measurement conducted by an experiment with a thin (0.2 atoms/barn) target optimized for higher cross-sections. This gives rise to significant uncertainty in the interaction length of neutrons in liquid argon. This paper presents results from the Argon Resonance Transport Interaction Experiment (ARTIE) at the Los Alamos Neutron Science Center (LANSCE), the first dedicated experiment optimized for the small cross sections in this energy region via use of a thick (3.3 atoms/barn) target

INTRODUCTION

Liquid argon (LAr) is used in a wide range of particle physics experiments investigating neutrinos [1–4], dark matter [5, 6], and neutrinoless double beta decay [7, 8]. Achieving many of the scientific objectives sought by these experiments relies on understanding the transport of neutrons through LAr at a level of precision which has only recently emerged as a critical experimental requirement. The neutron-argon total cross section from the ENDF [9] evaluation has a destructive interference feature at 57 keV, which appears as a negative cross section dip around this energy, where interaction length in LAr, for a natural abundance of isotopes, is 30 m. This is important, as at this energy scale, neutrons only lose a small fraction of their kinetic energy in single elastic collisions with relatively massive argon nuclei. Thus, even neutrons with kinetic energy well above 57 keV have a significant probability of reaching the low cross section region with the resulting long interaction length. The results of the most recent previous measurement [10], contained in the EXFOR database [11], are inconsistent with ENDF evaluation in the region of this feature, with an inferred interaction length of 4.2 m. This discrepancy makes it impossible to reliably predict the performance of LAr in transporting and shielding neutrons. For example, in large detectors like DUNE [12], neutrons from neutrino interactions will exit the detector volume at an uncertain rate and affect the energy resolution, while unwanted background neutrons will enter from the outside and become an uncertain background for solar and supernova neutrino measurements. Likewise, detector calibration systems which use externally-produced neutrons

rely critically on the penetration depth of neutrons into the inner volume for efficient operation [13].

This paper describes the Argon Resonant Transport Interaction Experiment (ARTIE) which was designed for the sole purpose of resolving the discrepancy. The transmission $T(E)$ is defined as the fraction of neutrons in a medium which pass through a distance d without scattering. This is related to the cross section by the equation:

$$\sigma(E) = -\frac{m_{Ar}}{\rho_{eff}d} \ln T(E) \quad (1)$$

Where m_{Ar} is the mass of an argon atom, d is the target thickness, and ρ_{eff} is the effective density. The ARTIE target was designed with a thickness approximately twenty times larger than used in Ref. [10]. Using ARTIE's higher thickness, the inconsistent cross section values reported by ENDF and Ref. [10] will result in a discrepancy of 20% in $T(E)$ at the dip energy around 57 keV. While well-suited to the dip region, the target quickly becomes opaque to neutrons at higher cross sections and which defines our energy Region Of Interest (ROI) to be 20 to 70 keV.

EXPERIMENTAL METHOD

The ARTIE target consisted of a column of LAr of length 168 cm and diameter 25 mm, held at atmospheric pressure, and contained in a vessel constructed from standard components. The target was inserted into Flight Path 13 (FP13) of the Lujan Neutron Scattering Center [14] at a distance 31 m from the upper-tier liquid hydrogen moderator of the accelerator-driven pulsed neu-

tron source. The Mark III Target-Moderator-Reflector-Shield (TMRS) [15] is driven by an 800 MeV proton linac that produces a 250 ns triangular pulse at a rate of 20 Hz with a typical beam current of 80 μ A. This current is converted by a Current Transformer (CT) into counting signals, and the integrated counts for every one-minute period are recorded by a scalar during data taking. The beam neutrons are produced via spallation reactions inside a tungsten target. ARTIE neutron detection was located approximately 30 m downstream of the target and consisted of a 9 cm diameter by 1 mm thick ^6Li -glass scintillator, viewed edge-on by two RCA 8854 five-inch photomultiplier tubes (PMTs). A DAQ trigger event was defined as a pulse above threshold in either PMT. The data acquisition system (DAQ) recorded a timestamp (used to calculate kinetic energy) and integrated charge for each neutron event.

Two-inch thick brass cylinders with 6 mm holes in the center were used to collimate the beam through the target. Two collimators were located upstream of the target, and two downstream. These constrained the beam to the center of the 25 mm diameter target, and produced a beam spot with an 8 cm diameter at the 9 cm diameter neutron detector.

Final alignment of the collimators was performed by first maximizing the DAQ-reported event rate. Collimators were then fine-tuned in order to produce a symmetric, fully contained image on storage-phosphor image plates at the detector location.

For insulation the target was covered with a rigid foam designed for cryogenic applications. Near each end an upward opening feeds into commercial nalgene dewars. As argon boiled in the target, Gaseous Argon (GAR) vented through the openings and was replaced by LAr from the dewars. During operation, dewars were refilled about once per hour to ensure that the target remained full. Data was collected during a two week period, with most runs being in either *target-in* (LAr fill) or *target-out* (GAR fill) mode. The use of GAR during target-out runs was accounted for by defining the effective target density as $\rho_{\text{eff}} = \rho_{\text{in}} - \rho_{\text{out}}$. The transmission was then experimentally determined as:

$$T(E) = \frac{N_{\text{in}}(E) - B_{\text{in}}}{N_{\text{out}}(E) - B_{\text{out}}} \cdot \frac{Q_{\text{out}}}{Q_{\text{in}}} \quad (2)$$

where $N_{\text{in/out}}$ is the number of neutrons observed in the neutron detector during target-in/out runs, $Q_{\text{in/out}}$ is the time integrated beam current as determined from the CT monitor, and $B_{\text{in/out}}$ is the experimentally determined background rate.

The collected data was subjected to both run quality and individual event selection cuts. Firstly, to minimize the impact of potential non-linearity between the CT sensor and the neutron beam intensity, the analysis only included the 95% of collected data taken while the CT was near the maximum value. Secondly, data taken

around the time of target filling were rejected since during these times, a roughly 30% excursion in the beam-intensity normalized neutron event rate was observed, which we surmise was caused by the unavoidable spilling of LAr vapor unto the brass collimators from the filling dewar located above them. The rate returned to the nominal value about 15 minutes after the end of the fill. Thus, these filling times were removed from the analysis by requiring that post-fill rate return to at least 95% of the pre-fill plateau value. This cut removed about 12% of the target-in data. Thirdly, both detector PMTs were required to have pulses within a 100 ns coincidence window, and to pass a cut which removed re-triggered events (*i.e.* two triggers from a single event). This last cut removed a negligible number of actual signal events. Following these cuts, there were 197k events recorded in the ROI for target in runs, and 85k for target out.

CALIBRATION

Energy: The neutron detector recorded a neutron time (t_n) and the proton beam pulse provided a start time (t_0). Together these gave a time-of-flight (TOF) which was used to determine the velocity (v) and hence the kinetic energy (E) of each event. These times were corrected for the average time a neutron scattered inside the moderator (t_{mod}), usually referred to as the *Moderator Function* (MF). The MF had been previously determined for LANSCE via Monte Carlo simulation [15]. In the ROI the MF correction is typically 1-2% with a smearing of about 10% about the mean. The ENDF predictions for neutron transmission and cross section are smeared by applying a Monte Carlo simulation using the MF. The velocity v is then a function of the TOF $t \equiv t_n - t_0$:

$$v(t) = \frac{L_{\text{fit}}}{t - t_{\text{mod}}(t) + t_{\text{fit}}} \quad (3)$$

where L_{fit} and t_{fit} were parameters determined by fitting features in the LAr data to known resonances of aluminum and cadmium (both present in the beamline) and argon. The best fit value of L_{fit} was 63.82 ± 0.06 m which agrees well with physical measurements made along the beam line. The parameter t_{fit} (best fit 420 ± 29 ns) accounted for time delays in the detector, cables, and DAQ, as well as any residual difference between the actual and simulated moderator response. In addition to the moderator time-smearing, the incident triangular-shaped neutron pulse had a FWHM of 125 ns which led to a 53 ns uncertainty in t_0 . These two factors dominated the energy resolution.

Target Density: Since the LAr in the target was always slightly boiling, there was always a small fraction of GAR present, which affected the overall target density. Thus, a separate experiment to directly measure the density of the liquid-gas mixture *in situ* was performed. The mass

of the target assembly (M) as a function of dewar liquid height (h) is given by:

$$M(h) = M_0 + (\rho_{eff} - \rho_{air}) V(h) \quad (4)$$

where ρ_{eff} is the effective density of the argon mixture, ρ_{air} is the density of air, M_0 is the mass of the empty target, and $V(h)$ is the volume of the target as a function of liquid height. M_0 was measured using a precision scale (± 1 g in the range of the roughly 25 kg target assembly mass), and $V(h)$ was determined by filling the target with known amounts of water and noting the level on a steel ruler inside the dewar. The dry, empty target was then filled with liquid argon while sitting on the precision scale. During the subsequent boil off, a camera was used to simultaneously record the scale mass M and the liquid level h , which were then analyzed to give $M(h)$. Note that the observed boil off rate of 1.56 L/hr was consistent with that observed during the neutron beam runs.

The thermal contraction of the system with LAr was calculated to have an insignificant effect on this measurement, but two small corrections were made in the analysis: (i) M was adjusted by 75 g to account for ice buildup on the target during the test, and (ii) a 1.3% upward adjustment in LAr density was made to account for the difference in density at the altitude of Los Alamos (2300 m) as compared to the lab where the density test was performed (16 m). An target-in density of $\rho_{in} = 1.318 \pm 0.017 \text{ g/cm}^3$ was obtained. This is 5.9% lower than the nominal density [16] of pure liquid phase, and implies that this fraction of argon gas was mixed in the target during the beam runs. This resulted in an effective density $\rho_{eff} = 3.3 \pm 0.04$ atoms/barn. The uncertainty in the density measurement was taken into account when calculating the overall experimental uncertainty.

BACKGROUNDS AND UNCERTAINTIES

Backgrounds: Determination of the argon transmission from Eq. 2 relied on subtracting background events, especially for the GAr runs. Many sources of backgrounds were considered: (i) Data collected while the beam was off or when the iron shutter was closed and the beam on indicated that these backgrounds were negligible, (ii) background from the “wrap-around” of slow neutrons from a previous pulse was effectively eliminated by the addition of a 0.16 cm thick cadmium filter, which strongly suppressed neutrons with kinetic energy below 0.5 eV, (iii) background from scattered beam neutrons that lose their original TOF correlation with energy, (iv) background from prompt moderator gammas that penetrate all the way to the neutron detector arrive too early to be significant in the ROI, and (v) background from delayed gammas from neutron capture in the water moderator,

which would produce a background nearly flat in TOF across the ROI, but still possible for GAr.

To measure these backgrounds, a standard technique [17][22] that utilizes resonances that scatter or absorb nearly all incident neutrons was used. Dedicated runs were made with a 2.54 cm thick aluminum filter inserted into the beamline which increased the attenuation of beam neutrons at the resonance energies of 5.9, 35 and 88 keV, which were already present due to the aluminum components in the moderator and beamline windows. The background was then extracted at the resonance energy by subtracting the expected counts given the calculated aluminum transmission from the observed counts, given by

$$B_{NF}(E) = \frac{N_F(E) - N_{NF}(E)T(E)}{R_{F/NF}(E) - T(E)} \quad (5)$$

where $T(E)$ is the ENDF-smearred transmission of neutrons with one filter applied, $N(E)$ are the counts in the bins at the resonance dips at 5.9, 35, and 88 keV for the one-filter case (F) and non-filter case (NF), and $R_{F/NF}(E)$ is the ratio of one-filtered background to the non-filter background. This ratio is introduced to correct background reduction due to filter attenuation. If the filter attenuation effect is negligible, this ratio can be approximated to be one.

Our method is based on the assumption that the neutron background at a given TOF is due to neutrons that arrive earlier which then scatter in the detector hall and are detected at random later times. This background is seen to be flat in time within our ROI [20] for our neutron beam. As the filter attenuation effect is non-negligible for the 2.54 cm aluminum filter, it is corrected by $R_{F/NF}(E)$ using an external measurement of the background components from [20] and private communication with the authors [21]. The ratio is $R_{F/NF}(E_{ROI}) = 0.755^{+0.021}_{-0.004}$, with total uncertainties determined by applying Eq. 5 for situations when $B_{NF}(E)$ consists entirely of gammas or neutrons.

For LAr fill runs, gammas from the moderator were heavily suppressed due to target thickness. A small background still remained, and thus an argon resonance at 77 keV was used to evaluate this near the ROI. This background was also expected to be flat in TOF.

Fig. 1 shows the GAr and LAr event rates as a function of TOF and energy. The background rates are fit to a constant resulting in a background contribution relative to the signal in the ROI of about 0.14% for LAr and 7.1% for GAr, where the one-sigma uncertainties (dotted lines) are given by the flat fit to all background measurements.

Long-term Beam Line Stability: The cross section calculation relies on the proportional nature between neutrons detected and the total integrated beam current, yet other than the ^6Li detectors at the end of the beam line, there is no monitor of the neutron flux once the proton

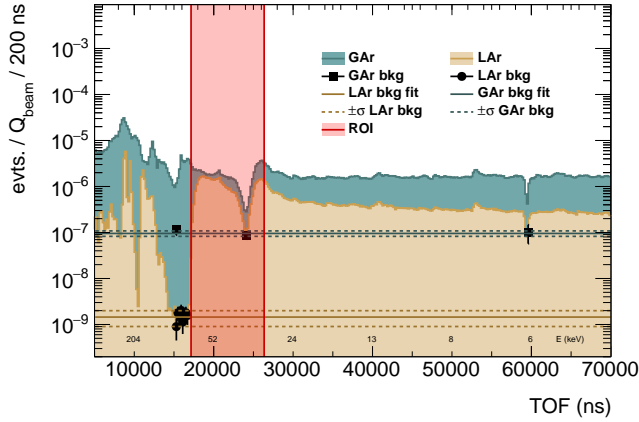


FIG. 1. The event rates and energy for a LAr and GAr filled target as a function of TOF. Filled points are the extracted background rates. Open points at high energy are used as a consistency check for LAr.

beam strikes the tungsten target. Since air and LAr data runs involve different target setups, the uncertainties associated with the neutron beam in the target hall, after the neutrons are created, are not cancelled naturally in Eq. 2. To assess these uncertainties, event rates normalized by beam current were analyzed as a function of time for both air and LAr data, discussed below.

Air: Air data, due to similar densities and neutron cross sections, was used as a surrogate for long term beam line stability of GAr data. This assessment includes any systematic effects from changing atmospheric pressure. Three days of air data showed a daily modulation correlated closely to outside air temperature, and consistent across energies below, within, and above our ROI. Due to the close correlation to temperature, we suspect the effect is due to misalignment from the thermal expansion and contraction along the entire length of the beam line. The combined uncertainty on median air event rate is taken as an asymmetric systematic of +3.14% and -3.93% [19].

LAr: LAr data did not show the same modulation as the air data. A measurement of the event rate as a function of time for LAr includes event rate decrease from ice build-up on the kapton windows and also the cuts used to remove periods of refilling. The combined uncertainty on median LAr event rate is taken as an asymmetric systematic of +0.69% and -1.06% [19].

Target Density: As described in the calibration section, this was measured with a systematic uncertainty of 1.3%.

After the selection cuts, several other systematic uncertainties were determined to be negligible, including those from: non-linearity between the beam intensity and CT measurement, dead time in the DAQ system [19], PMT afterpulsing [19], and contamination of the argon gas.

The absolute energy calibration was limited by the statistical uncertainties on the fitted parameter $\delta(t_{\text{fit}}) =$

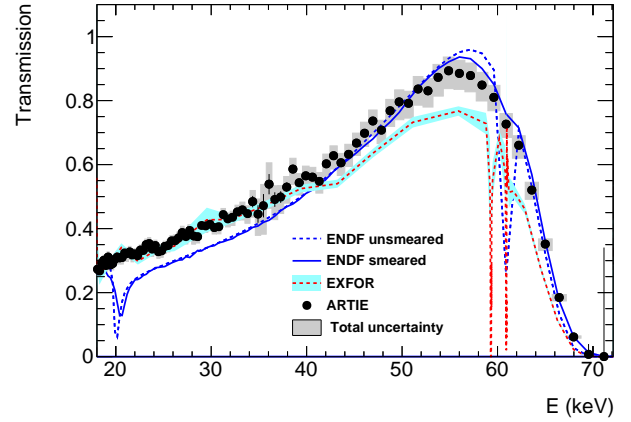


FIG. 2. The measured transmission of argon compared to EXFOR[11] and ENDF. The black points are data with statistical uncertainties. For most energies, statistical error bars are smaller than the symbols.

29 ns, and the contribution from $\delta(L_{\text{fit}}) = 0.064$ m was negligible. No systematic uncertainty for energy resolution was applied to the cross section results, which are reported here as a function of measured energy.

The total systematic uncertainties on transmission and cross section are estimated for each energy point by using a toy Monte Carlo simulation where all relevant parameters are allowed to vary simultaneously around their central values. The resulting spreads within the 68 percentile around the central-value measurements of transmission and cross section are taken as the total systematic uncertainties.

CONCLUSIONS

From the neutron counts in each TOF bin, the transmission T is calculated from Eq. 2 and the cross section from Eq. 1. The central value of each TOF bin is converted to energy using Eq. 3. Fig. 2 shows the transmission as a function of energy for the range 20-70 keV. The measured neutron-argon total cross section as a function of kinetic energy is shown in Fig. 3. The points are the central values and the bars represent the statistical uncertainty. The shaded grey regions are the total uncertainty, which includes systematic uncertainties. The dashed red and blue lines represent the EXFOR database [11] and ENDF evaluation, and the solid blue line is the ENDF prediction smeared by the expected ARTIE energy resolution. The beam energy resolution does not allow us to see the sharp features near 60 keV. It can be seen that, for energies below 40 keV ARTIE data is in good agreement with the EXFOR database with data obtained from previous measurement [10], while the ENDF evaluation shows slightly higher cross sections. Between 40 and 70

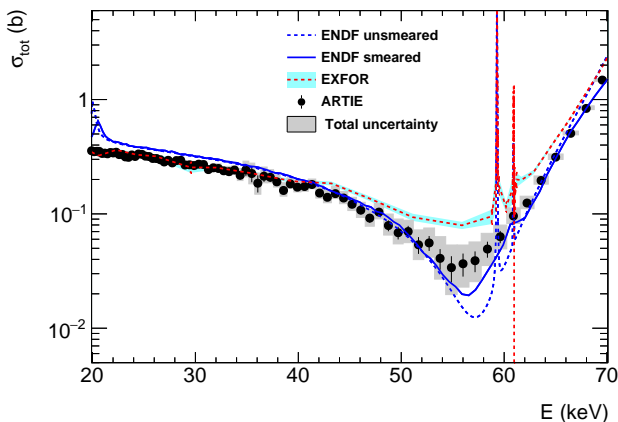


FIG. 3. Neutron-argon total cross section as a function of energy. Also shown are the EXFOR evaluation and the ENDF evaluation smeared by the ARTIE energy resolution.

keV, ARTIE data is in better agreement with the ENDF evaluation, confirming the existence of the low cross section dip. As a cross check of our experimental setup and analysis technique, the transmission for carbon was measured from data collected with two 0.125 ± 0.010 " thick carbon (99.999% purity) disks [18] attached to the target while filled with GAr. There was good agreement between the measured ($0.73^{+0.03}_{-0.05}$) and predicted (0.72) transmission in the ROI with $\chi^2/\text{NDF} = 2.7/6$, which served as a validation for much of the ARTIE analysis.

In conclusion, our results confirm a dip in the total cross section between 50 and 60 keV. The data point at 54.9 keV is found to have the lowest cross section of $\sigma = 0.0339 \pm 0.0087_{\text{stat}-0.0112_{\text{sys}}}^{+0.0175_{\text{sys}}} = 0.0339^{+0.0195}_{-0.0142} \text{ barn}$. These results have significant implications on the ability to reliably predict neutron transport to the level required in rare event neutrino and dark matter experiments using liquid argon, as neutrons that fall into this dip region can be transported for long distances in liquid argon, giving rise to potential backgrounds in rare event searches.

ACKNOWLEDGEMENTS

Work at UC Davis was supported by the U.S. Department of Energy (DOE) Office of Science under award number DE-SC0009999, and by the DOE National Nuclear Security Administration through the Nuclear Science and Security Consortium under award number DE-NA0003180. Support for LIP was from the Fundação para a Ciência e a Tecnologia, I.P., project CERN/FIS-PAR/0012/2019. Major support was also provided by the U.S. Department of Energy through the Los Alamos National Laboratory. Los Alamos National Laboratory is operated by Triad National Security, LLC, for the National Nuclear Security Administration of U.S. Depart-

ment of Energy (Contract No. 89233218CNA000001). Finally, we gratefully acknowledge the logistical and technical support and the access to laboratory infrastructure provided to us by LANSCE and its personnel.

BIBLIOGRAPHY

- [1] M. Antonello et al. ICARUS at FNAL. 2013.
- [2] R. Acciarri et al. Design and Construction of the Micro-BooNE Detector. *JINST*, 12(02):P02017, 2017.
- [3] B. Abi et al. The Single-Phase ProtoDUNE Technical Design Report. 2017.
- [4] R. Acciarri et al. Long-Baseline Neutrino Facility (LBNF) and Deep Underground Neutrino Experiment (DUNE) Conceptual Design Report, Volume 4 The DUNE Detectors at LBNF. 2016.
- [5] C. E. Aalseth et al. DarkSide-20k: A 20 tonne two-phase LAr TPC for direct dark matter detection at LNGS. *Eur. Phys. J. Plus*, 133:131, 2018.
- [6] R. Ajaj et al. Search for dark matter with a 231-day exposure of liquid argon using DEAP-3600 at SNOLAB. *Phys. Rev. D*, 100:022004, 2019.
- [7] K. H. Ackermann et al. The GERDA experiment for the search of $0\nu\beta\beta$ decay in ^{76}Ge . *Eur. Phys. J.*, C73(3):2330, 2013.
- [8] N. Abgrall et al. The Large Enriched Germanium Experiment for Neutrinoless Double Beta Decay (LEGEND). *AIP Conf. Proc.*, 1894(1):020027, 2017.
- [9] D. A. Brown et al. ENDF/B-VIII.0: The 8th Major Release of the Nuclear Reaction Data Library with CIELO-project Cross Sections, New Standards and Thermal Scattering Data. *Nucl. Data Sheets*, 148:1–142, 2018.
- [10] R.R. Winters, R.F. Carlton, C.H. Johnson, F.W. Hill, and M.R. Lacerna. Total cross section and neutron resonance spectroscopy for $n + ^{40}\text{Ar}$. *Phys. Rev. C*, 43:492, 1991.
- [11] V.Semkova N.Otuka, E.Dupont et al. Towards a More Complete and Accurate Experimental Nuclear Reaction Data Library (EXFOR): International Collaboration Between Nuclear Reaction Data Centres (NRDC). *Nuclear Data Sheets*, 120, 2014.
- [12] B. Abe and others. Deep Underground Neutrino Experiment (DUNE), Far Detector Technical Design Report. FERMILAB-PUB-20-025-ND. 2020.
- [13] Babak Abi et al. Deep underground neutrino experiment (dune), far detector technical design report, volume iv far detector single-phase technology. *arXiv: Instrumentation and Detectors*, 2020.
- [14] P.W. Lisowski, C.D. Bowman, G.J. Russell, and S.A. Wender. The Los Alamos National Laboratory Spallation Neutron Sources. *Nucl. Inst. and Meth.*, 106:208, 1990.
- [15] Lukas Zavorka, Michael J. Mocko, Paul E. Koehler, and John L. Ullmann. Benchmarking of the MCNPX Predictions of the Neutron Time-emission Spectra at LANSCE. American Nuclear Society, 20th Topical Meeting of the Radiation Protection and Shielding Division of ANS,

- 2018.
- [16] H.M. Roder. Liquid densities of oxygen, nitrogen, argon, and parahydrogen. *NBS Technical Note 361 (Revised)*, 1974.
 - [17] J.M. Brown, A. Youmans, N. Thompson, Y. Danon, D.P. Barry, G. Leinweber, M.J. Rapp, R.C. Block, and R. Bahran. Neutron Transmission Measurements and Resonance Analysis of Molybdenum-96. *AccApp '17*, 2017.
 - [18] Carbon (graphite) (c) sputtering targets. https://www.lesker.com/newweb/deposition_materials/depositionmaterials_sputtertargets_1.cfm?pgid=car1.
 - [19] T. Erjavec. *Understanding Neutron Transport for Liquid Argon Rare-Event Searches*. PhD thesis, University of California Davis, Davis, CA, 2024.
 - [20] A. Stamatopolous, P. Koehler, A. Couture, B. DiGiovine, G. Rusev, and J. Ullmann. New capability for neutron transmission measurements at LANSCE: The DICER instrument. *NIM A '22*, 2022.
 - [21] P. Koehler. Private Communication, 2022.
 - [22] R. Mucciola, C. Paradela, G. Alaerts, S. Kopecky, C. Massimi, A. Moens, P. Schillebeeckx, and R. Wynants. Evaluation of resonance parameters for neutron interactions with molybdenum. *Nuclear Instruments and Methods in Physics Research Section B: Beam Interactions with Materials and Atoms*, 531:100–108, 2022.